

QUENCH TEXTURES IN BASALTIC DYKE FROM SCHIRMACHER OASIS, QUEEN MAUD LAND, EAST ANTARCTICA

S. H. Jafri

National Geophysical Research Institute, Hyderabad

j

Abstract

Occurrence of several morphologies of quench olivine textures in a basaltic dyke is reported from Antarctica for the first time. This basaltic dyke occurs in the Precambrian polymetamorphosed gneissic terrian of Schirmacher Oasis, Queen Maud Land, East Antarctica. The morphologies of quench olivines in this basaltic dyke suggest that they were formed by rapid cooling of the magma at 15-40° c/hour. Further, the delicate nature of the quench olivine, which are mostly confined to the glassy margins of the dyke suggest their insitu crystallisation.

Introduction

Quench textures have been described in submarine basalts (Muir and Tilley, 1966; Bryan, 1972; Jafri and Charan, 1992), Lunar basalts (Basaltic Volcanism Study Project, 1981; Lofgren, 1971) and basic - ultrabasic rocks (Gelinas and Brooks, 1974; Fleet, 1975). They have also been produced experimentally and it is suggested that the crystal forms depend on the cooling or supercooling rates of the magmatic liquids (Lofgren, 1974, 1980, Donaldson, 1976) By comparing the shapes of crystals produced in such experiments with those observed in the natural rocks of a similar composition, it is possible to deduce the approximate rate(s) of cooling at which the crystal nucleated and grew in the rocks

(Donaldson, 1976). In this study a basaltic dyke which is characterised by the occurrence of several morphologies of quench olivine textures, is being reported from Schirmacher Oasis, Queen Maud Land, East Antarctica.

Geology

The Schirmacher Oasis is composed of polyphase gneiss (Garnet-biotite gneiss, Augen gneiss, Quartzo-feldspathic gneiss, Streaky gneiss and Calc gneiss) with minor intercalations of banded gneiss, calc silicates and amphibolites (Hussain and Diwakara Rao, 1996, Sengupta, 1988) Rb-Sr dating reveals 853 ± 51 Ma age for Garnet-biotite gneiss and 773 ± 26 age Ma for Quartzo - feldspathic gneiss (Rama Rao et al., 1995). The rocks were tectonically disturbed and show high to medium grade metamorphism and exhibit multiple deformation (Bormann et al., 1986; Sengupta, 1988). The post-metamorphic intrusives consists of pegmatites, lamprophyres, aplites and basaltic dykes. Few basaltic dykes of the Oasis range in age (K-Ar) from 290 ± 4 Ma to 302 ± 10 Ma (Kaiser and Wand, 1985), while the ages (Rb-Sr) of lamprophyres are 455 ± 12 Ma (Dayal and Hussain, 1997).

The basaltic dyke reported here, trends NNW-SSE and intrudes the E-W foliated garnet-biotite gneiss, a major rock formation of Schirmacher Oasis, suggesting that the dyke emplacement is a Late Proterozoic/Phanerozoic event. It is about 1 meter across and is traceable over a length of about 100 meters. It is fine grained, aphyric and characterised by chilled margins.

Crystal Morphology

The mineral assemblage in the dyke rock consists of olivine, plagioclase, clinopyroxene, titanomagnetite and glass. The olivine (F_{078-85}) occurs as microphenocrysts and shows several morphologies of quench textures (Fig.1 a, b, c, d, e). These olivine microphenocrysts, which are mostly confined to the glassy margins of the dyke are slightly altered and are partially replaced by talc and chlorite. Clinopyroxene is augite and occurs both as microphenocrysts and interstitial grains and shows partial alteration to

chlorite and epidote. Away from the margins and towards interior of the dyke, the grain size increases and development of subophitic texture is noticed. Plagioclase (An_{53-58}) occurs mainly as microlites and also as microphenocrysts. The plagioclase microphenocrysts are partially saussuritised.

Mineral compositions were determined from well-polished and carbon-coated thin sections by using a Camebax-Micro WDS electron probe microanalyses. Accelerating voltage was 15-kV, beam currents 4 to 6 nA, counting time 10 seconds and beam diameter 1-5 μ m, utilizing the online ZAF correction procedure of Bence and Albee (1968), in comparison with suitable natural and synthetic mineral standards. The mineral compositions are given in Table 1, 2 and 3.

Geochemistry

Representative rock samples of the dyke were analysed for major and minor elements using a Philips PW-1400 model X-ray Fluorescence Spectrophotometer. Precision and accuracy of XRF data have been reported in detail elsewhere (Govil, 1985). Trace and rare earth elements (REE) were determined using ICP-MS (VG Plasma Quad) technique and precision and accuracy of data have been reported by Balaram et. al. (1992). Analytical data presented here have a reproducibility of measurements better than $\pm 7\%$ RSD for all the trace and rare earth elements.

The major, minor and trace element compositions of the dyke samples are given in Table 4. The major and trace element composition (SiO_2 , ranging from 46.80 to 47.50%) is reasonably distinctive as these are characterised by high abundance of K, Rb, Ba, Zr, P and Ti. The light rare earth elements concentrations range from 42-44 times chondritic values and heavy rare earth elements from 8-9 times chondritic (Fig.2). They have high FeO/MgO ratios (range 2.10 - 2.28), which is a characteristic indicator of advanced fractional crystallization (Miyashiro, 1974, 1975; Miyashiro and Shido, 1975; Tatsumi and Ishizaka, 1982).

This dyke resembles an alkali basalt in composition (Fig.3)

and in other oxide contents, such as P_2O_5 vs Zr and TiO_2 vs Zr/ P_2O_5 relationships (Figs 4, 5). The samples exhibit negative Nb anomalies (Fig.6)

Discussion

The elemental composition of the basaltic dyke from Schirmacher Oasis, suggest that it is an alkalic basalt (Figs. 3,4,5) and derived from a mantle source. The LREE enrichment ($La_n/Yb_n = 4.39-5.43$) and negative Nb anomalies in the dyke samples suggest that the source magma was fractionated and contaminated with crustal rocks during its ascent through the continental crust.

This dyke is also characterised by the occurrence of quench olivine textures that are similar to those reported from submarine basalts, lunar basalts and experimentally produced quench olivine textures (Basaltic Volcanism Study Project, 1981). Olivine crystals can adopt 10 type of shapes and experimental crystallisation of rock melts shows that there is a systematic change from polyhedral or granular olivines - hopper olivines - branching olivines etc., with increase in cooling rate and with increase in degree of supercooling (Donaldson, 1976)

The morphologies of quenched olivines, which occur in this basaltic dyke are externally subhedral to euhedral hoppers, with marked internal skeletal characters (Figs.1 a, b) and also as externally euhedral and internally hollow elongate hoppers, with marked edge growth (Figs.1 c, d, e), thus suggesting that these olivine textures were produced by rapid cooling of the source magma by about $15-40^\circ$ c/h. Further, the delicate nature of these skeletal olivine crystals seems to preclude transport and may have crystallised insitu from the liquid (Berg and Klewin, 1987). The occurrence of skeletal textures (Fig.1) mostly confined to the margins of the dyke also supports their insitu crystallisation.

Acknowledgements

The author is grateful to Dr. H. K. Gupta, Director, N.G.R.I. Hyderabad and. Secretary, DOD, New Delhi, for sponsoring his participation in the 17th Indian Scientific Expedition to Antarctica and permission to publish this paper. The author is thankful to Dr. V. Diwakara Rao for discussions and valuable suggestions.

REFERENCES

- Balaram, V., Manikyamba, C, Ramesh, S.L. and Anjaiah, K V. (1992) Rare earth and trace elements determination in iron formation reference samples by ICP-MS. *Atomic Spectroscopy*, V.13, pp.13-25
- Basaltic Volcanism Study Project (1981). *Basaltic Volcanism on the Terrestrial Planets*. Pergamon Press. Inc., New York. 1286pp.
- Bence, A.E. and Albee, A.L. (1968). Empirical correction factors for the electron microanalysis of silicates and oxides. *Jour. Geol.*, V.76, pp.382-403
- Berg, J.H. and Klewin, K.W. (1988) High - MgO lavas from the Keweenawan midcontinent rift near Mamainse Point, Ontario. *Geology*, V.16, pp-1003-1006
- Bormann, P., Bankwitz, P., Bankwitz, E., Damm, V., Hurting, E., Kampf, H., Menning M., Peach, H.J., Schafer, U. and Stackebrandt, W. (1986), Structure and development of the Passive continental margin across the Princess Astrid Coast, East Antarctica, *Jour, Geodyn*, V6, pp. 347-373
- Bryan, W.B. (1972). Morphology of quench crystals in submarine basalts. *Jour, Geophy, Research.*, V.77, pp.5812-5819.
- Dayal, A.M. and Hussain, T.S.M. (1997) Rb-Sr ages of lamprophyre dykes from schirmacher Oasis, Queen Maud Land, East. Antarctica. *Jour. Geol. Soc.India*. V.50 pp.457-460
- Donaldson, C.H. (1976). An experimental investigation of olivine morphology. *Contr. Mineral. Petrol.*, V.57, pp. 187-213
- Fleet, M.E. (1975). Growth habits of clinopyroxenes. *Canad. Mineral.*, V.13, pp-336-341.
- Gelinas, L. and Brooks, C. (1974). Archaean quench-texture tholeiites. *Canad. Jour. Earth Sci.*, V.11, pp-324-340.
- Govil, P.K. (1985). X-ray fluorescence analysis of major, minor and selected trace elements in new IWG reference rock samples.

Jour Geol. Soc. India, V.26. pp. 38-42.

Hussain, T.S.M. and Diwakara Rao, V. (1996). Geochemistry of polyphase gneisses from Schirmacher Oasis, East Antarctica. Jour. Geol. Soc. India. V.47, pp.303-312.

Jafri, S. H. and Charan, S. N. (1992). Quench textures in pillow basalts from the Andaman-Nicobar Islands. Bay of Bengal, India. Proc. Indian Acad. Sci. (Earth Planet Sci.) V.101, pp. 99-107.

Kaiser, G. and Wand, U (1985). K-Ar dating of basalt dykes in the Schirmacher Oasis area, Dronning Maud Land, East Antarctica; Zeit, Geol, Wissensch., Berlin V.13, pp. 299-307

Lofgren, G. (1971). Spherulitic textures in glassy and crystalline rocks. Jour. Geophys. Res. V. 76, pp. 5635-5648.

Lofgren, G. (1974). An experimental study of plagioclase crystal morphology; Isothermal crystallisation. Am Jour. Sci., V.274 pp.243-273

Lofgren, G. (1980) Experimental studies on the dynamic crystallisation of silicate melts. In : Physics of magmatic Processes (ed.) R.B.Hargraves, Princeton Univ. Press. New Jersey pp. (487-543)

Miyashiro, A (1974). Volcanic rock series in island arcs and active continental margins. Am. Jour Sci., V. 742, pp. 321-355.

Miyashiro, A (1975). Classification, characteristics and origin of ophiolites. Jour Geol, V.83, pp.249-281.

Miyashiro, A and Shido, F (1975). Tholeiitic and calc-alkalic series in relation to the behaviour of titanium, vanadium, chromium and nickel. Am. Jour Sci., V.275, pp.265-277

Muir, I.D. and Tiiley, C.E. (1966). Basalts from the northern part of the Mid-Atlantic Ridge, The Atlantic collection near 30 N., Jour, Petrol., V.7, pp. 193-201.

Rama Rao P., Ramana Rao, A.V. and Poornchandra Rao, G.V.S. (1995). Geological, Geochemical, Geochronological and Paleomagnetic studies on the rocks From parts of East Antarctica. Technical report No.8. Dept. Ocean Development. New Delhi, pp.97-106

Sengupta, S.S. (1988), Precambrian rocks of Schirmacher Range, East Antarctica. *Zeit. Geol. Wissensch.*, Berlin, pp.647-660

Sun, S.S. and McDonough, W.F. (1989). Chemical and isotopic signatures of ocean basalts. In : Saunders, A.D. and Norry,

M.J. (eds.), *Magmatism in the Ocean Basins*, Geol. Soc. Spec. Publ. N0.42, pp 313-345

Talumi Y and Ishizaka K. (1982). Origin of high Magnesian andesites in the Setoucli Volcanic belt, South West Japan, I. Petrological and chemical characteristics. *Earth Planet, Sci. Lett.* V.60, pp.293-304.

Figure Captions

Fig.1 (a, b, c, d, e) Photomicrograph of olivine microphenocrysts in glassy margins of basaltic dyke.

Fig. 2 : Chondrite-normalised REE pattern of basaltic dyke.

Fig. 3 : SiO₂ versus Na₂O+K₂O relationship of the dyke.

Fig. 4 : P₂O₅ versus Zr relationship of the dyke.

Fig. 5 : TiO₂ versus Zr/P₂O₅ relationship of the dyke.

Fig. 6 : Mantle normalised trace element abundance pattern for the basaltic dyke (mantle normalising values from Sun and McDonough, 1989)

TABLE 1 : MICROPROBE ANALYSIS OF OLIVINE.

	67/4	67/6	67/8	67/10	169/13	169/14
SiO ₂	37.90	38.41	38.59	37.93	42.15	40.66
TiO ₂	0.03	0.01	0.00	0.07	0.01	0.01
Al ₂ O ₃	0.03	0.06	0.04	0.02	0.00	0.01
FeO(T)	17.22	20.11	17.78	18.55	16.28	13.96
MnO	0.33	0.36	0.37	0.32	0.33	0.24
MgO	43.16	40.99	43.55	41.52	40.96	45.30
CaO	0.34	0.39	0.40	0.32	0.30	0.30
Na ₂ O	0.01	0.07	0.18	0.00	0.04	0.00
K ₂ O	0.12	0.03	0.02	0.07	0.04	0.06
Cr ₂ O ₃	0.35	0.05	0.00	0.08	0.10	0.11
NiO	0.26	0.14	0.10	0.15	0.14	0.31
	99.75	100.62	101.03	99.03	100.35	100.96
Cations on the basis of 4 Oxygens						
Si	0.972	0.986	0.977	0.983	1.055	1.007
Ti		0.001		0.000	0.000	0.000
Al		0.001		0.002	0.000	0.000
Fe ⁺²	0.369	0.432	0.376	0.402	0.341	0.289
Mn	0.007	0.008	0.008	0.007	0.007	0.005
Mg	1.650	1.568	1.643	1.604	1.527	1.672
Gl	0.009	0.011	0.011	0.009	0.008	0.008
Na	0.000	0.003	0.009	0.000	0.002	0.000
K	0.004	0.001	0.001	0.002	0.001	0.002
G	0.007	0.001	0.000	0.002	0.002	0.002
Ni	0.005	0.003	0.002	0.003	0.003	0.006
	3.026	3.015	3.027	3.015	2.946	2.992

Fo 82 78 81 80 82 85

TABLE 2 : MICROPROBE ANALYSIS OF PYROXENE.

	1	2	3	4	5	6
SiO ²	45.51	48.46	48.35	50.30	50.22	54.35
TiO ₂	2.84	1.10	1.29	0.63	1.31	0.81
Al ₂ O _a	8.03	6.86	6.90	4.21	8.57	4.36
FeO(T)	12.77	7.32	8.04	6.92	9.03	9.22
MnO	0.30	0.16	0.71	0.18	0.23	0.21
MgO	10.53	14.12	14.13	15.86	14.09	15.38
CaO	19.44	20.91	20.91	19.99	15.62	15.83
Na ₂ O	1.37	0.54	0.60	0.54	0.72	0.40
K ₂ O	0.11	0.04	0.05	0.03	0.03	0.04
Cr ₂ O ₃	0.00	0.68	0.24	0.17	0.46	0.02
NiO	0.01	0.04	0.00	0.03	0.02	0.04
	100.91	100.23	101.22	98.86	100.30	100.66
Cations on the basis of 6 Oxygens						
Si	1.724	1.797	1.785	1.877	1.834	1.966
Ti	0.081	0.031	0.036	0.018	0.036	0.022
Al	0.359	0.300	0.300	0.185	0.369	0.186
Fe+2	0.405	0.227	0.248	0.216	0.276	0.279
Mn	0.010	0.005	0.022	0.006	0.007	0.006
Mg	0.595	0.780	0.777	0.882	0.767	0.829
Ca	0.789	0.831	0.827	0.799	0.611	0.614.
Na	0.101	0.039	0.043	0.039	0.051	0.028
K	0.005	0.002	0.002	0.001	0.001	0.002
Cr	0.000	0.020	0.007	0.005	0.013	0.001
Ni	0.000	0.001	0.000	0.001	0.001	0.001
	4.068	4.033	4.048	4.030	3.965	3.934
Fs	22.64	12.35	13.39	11.39	16.68	16.20
En	33.26	42.44	41.95	46.49	46.37	48.14
Wo	44.10	45.21	44.65	42.12	36.94	35.66

TABLE 3 : MICROPROBE ANALYSIS OF PLAGIOCLASE.

	1	2	3	4	5	6
SiO ₂	53.17	54.55	53.40	53.09	52.43	53.11
TiO ₂	0.04	0.03	0.08	0.03	0.10	0.37
Al ₂ O ₃	30.28	27.11	30.08	29.45	29.42	27.86
FeO(T)	0.75	0.63	0.70	0.58	0.84	0.32
MnO	0.00	0.03	0.00	0.01	0.00	0.03
MgO	0.23	0.02	0.06	0.09	0.08	0.43
CaO	11.49	11.61	11.93	11.19	11.09	10.21
Na ₂ O	4.72	5.56	4.59	4.47	4.61	4.82
K ₂ O	0.33	0.41	0.28	0.27	0.29	0.42
Cr ₂ O ₃	0.07	0.00	0.00	0.00	0.04	0.00
Ni ^o	0.01	0.00	0.00	0.01	0.01	0.02
	101.09	99.95	101.12	99.19	98.91	97.59
Cations on the basis of 8 oxygens						
Si	2.388	2.483	2.397	2.421	2.404	2.458
Ti	0.001	0.001	0.003	0.001	0.003	0.013
Al	1.603	1.455	1.592	1.583	1.591	1.520
Fe ⁺²	0.028	0.024	0.026	0.022	0.032	0.012
Mn	0.000	0.001	0.000	0.000	0.000	0.001
Mg	0.015	0.001	0.004	0.006	0.005	0.030
Ca	0.553	0.566	0.574	0.547	0.545	0.506
Na	0.411	0.491	0.400	0.395	0.410	0.432
K	0.019	0.024	0.016	0.016	0.017	0.025
Cr	0.002	0.000	0.000	0.000	0.001	0.000
Ni	0.000	0.000	0.000	0.000	0.000	0.001
	5.002	5.046	5.012	4.992	5.010	4.998
Or	1.93	2.24	1.77	2.00	2.00	2.00
Ab	41.81	44.91	40.40	41.00	42.00	45.00
An	56.26	52.85	57.97	57.00	56.00	53.00

TABLE 4 : CHEMICAL COMPOSITION OF BASALTIC DYKE FROM SCHIRMACHER OASIS, EAST ANTARCTICA

	Ant-1	Ant-2	Ant-3	Ant-4
SiO ₂ (wt%)	46.80	47,50	47.20	47.30
TiO ₂	1.48	1.43	1.43	1.41
Al ₂ O ₃	14.10	13.98	13.90	13.85
Fe ₂ O ₃	7.93	7.54	7.38	7.35
FeO	5.36	5.28	5.36	5.28
CaO	9.33	9.23	9.04	9.04
MgO	5.94	5.41	5.26	5.28
Na ₂ O.	3.98	4.26	4.38	4.34
K ₂ O	1.43	1.40	1.39	1.36
MnO	0.54	0.61	0.52	0.59
P ₂ O ₅	0.46	0.45	0.45	0.43
LOI	1.06	1.23	2.30	2.54
Total	98.41	98.32	98.61	98.77
Ni (ppm) 84	61	101	84	
Cr	142	107	167	136
Rb	30	31	29	29
Sr	449	471	428	450
Y	19	20	29	30
Zr	75	79	79	83
Ba	547	599	520	540

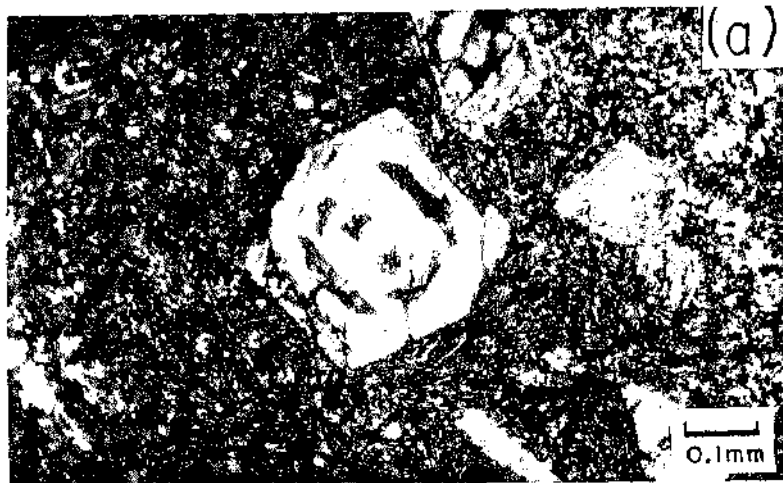


Fig -1 (a)



Fig -1 (b)

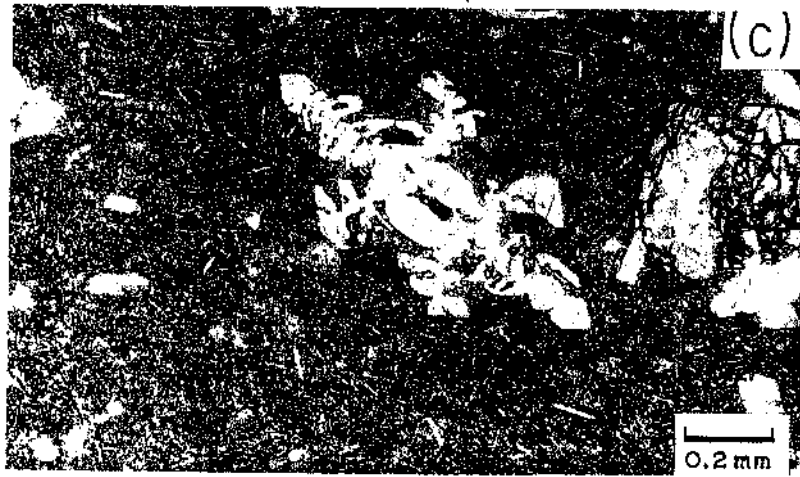


Fig -1 (c)



Fig -1 (d)



Fig -1 (e)

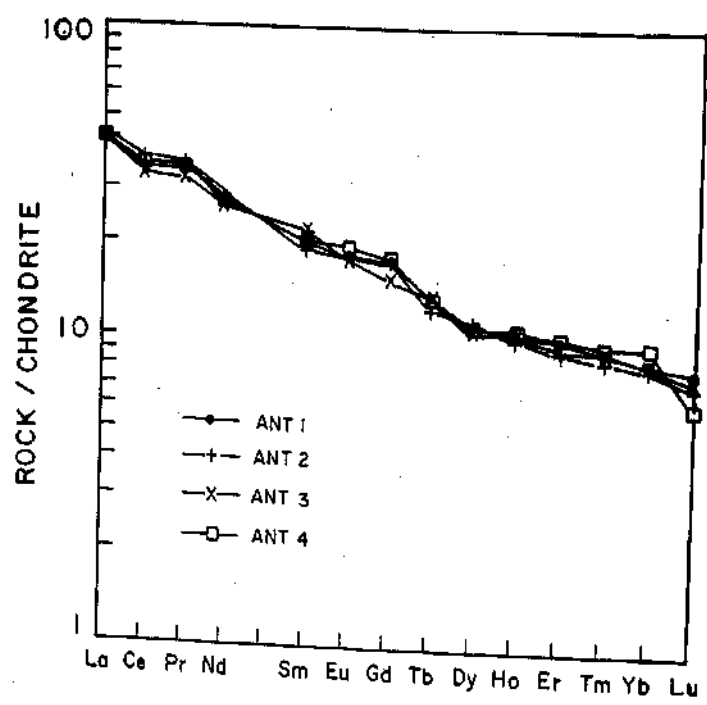


Fig - 2

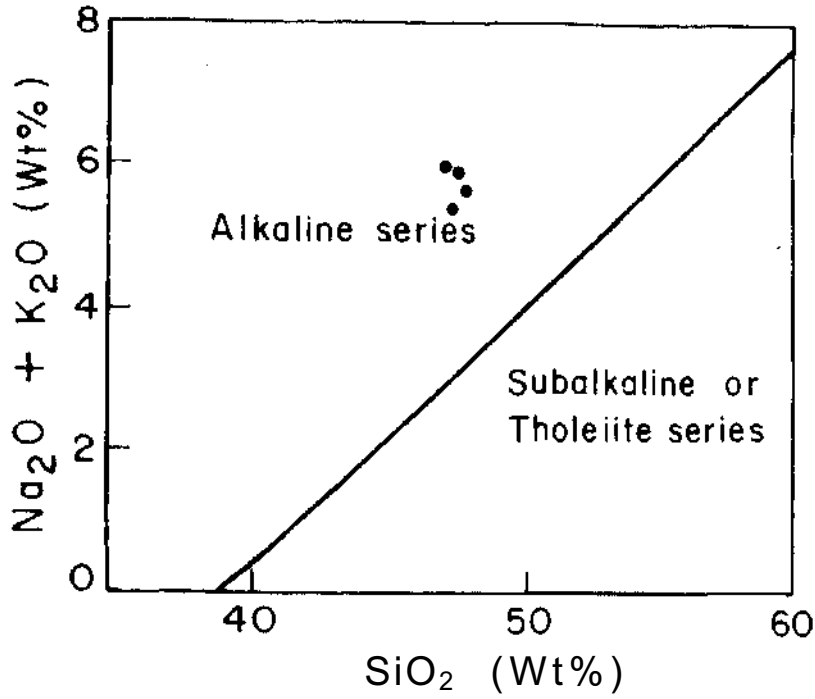


Fig - 3

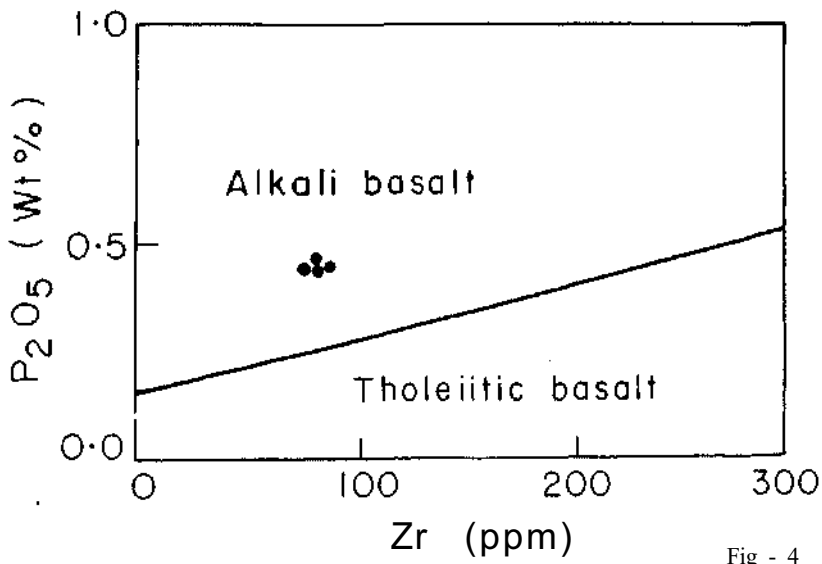


Fig - 4

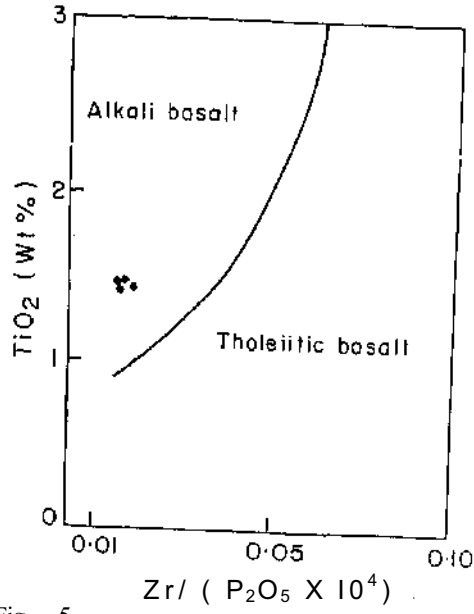


Fig - 5

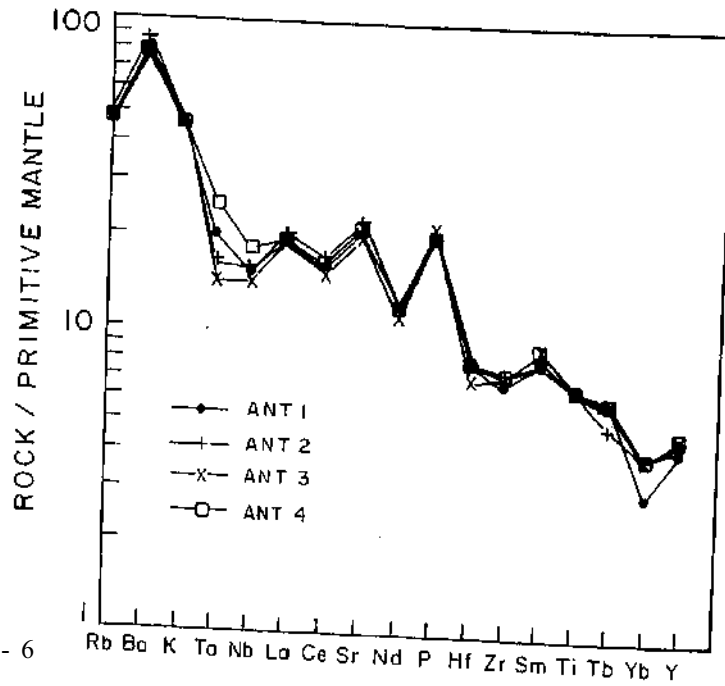


Fig - 6